Journal of Sound and Vibration (1999) **219**(3), 429–449
Article No. jsvi.1998.1845, available online at http://www.idealibrary.com.on IDEAL

ELECTROPNEUMATIC TRANSDUCERS AS SECONDARY ACTUATORS FOR ACTIVE NOISE CONTROL, PART II: EXPERIMENTAL ANALYSIS OF THE SUBSONIC SOURCE

L. A. BLONDEL†

Faculté Polytechnique de Mons, Laboratory of Acoustics, 9 rue de Houdain, B-7000 Mons, Belgium

AND

S. J. ELLIOTT

Institute of Sound and Vibration Research, The University of Southampton, Southampton SO17 1BJ, England

(*Received* 29 *July* 1997, *and in final form* 9 *July* 1998)

An experimental analysis of a subsonic compressed-air sound source has been carried out. The design of the source is described, in which a sliding plate which modulates the air flow is driven by an electrodynamic shaker. Friction between the sliding plate and its housing are reduced by coating their faces with glass-filled PTFE. The alternating acoustic pressure at the source output has been measured for various conditions. On the basis of these experimental results, the validity of the theoretical model derived in a companion paper is assessed. Predistortion of the subsonic source to produce a sinusoidal output is considered. A predistortion processor is placed in series with the electrodynamic shaker, the output of which is being computed on the basis of the fundamental equation of the subsonic compressed-air source. The measurement of the pneumatic efficiency of the source is also considered, by using a hot-wire anemometer for the measurement of the air flow across the source. The experimental results are found to be in good agreement with the theoretical predictions developed in the companion paper, Part I.

1. INTRODUCTION

A theoretical analysis of electropneumatic transducers was developed in a companion paper (Part I). The main conclusion was that electropneumatic sources were potentially good candidates for secondary sources in active noise control systems since they are ruged and capable of operating with high efficiencies. The analysis revealed that the pneumatic efficiency of these sources was very large compared to that of a sonic electropneumatic source, and was even larger than the electro-acoustic efficiency of electrodynamic loudspeakers. The theoretical

†Present address: ALSTON, Signolling Group, B.P. 4211, B-6001, Charleroi, Belgium.

0022–460X/99/030429 + 21 $30.00/0

analysis also showed, however, that unlike sonic electropneumatic sources, the subsonic transducer was a non-linear device, at least when used as a conventional acoustic generator. In this case, the source can be linearized by using a predistortion processor. When the transducer is connected to a small acoustic impedance, which is generally the case when the source is acting in an active noise control system, the source non-linear behaviour is strongly reduced. An experimental analysis of the sonic electropneumatic source was presented by Glendinning *et al*. [1]. A gas bearing was used by these authors to support the friction-free motion of a sliding plate which modulated the supply of compressed air. The main conclusion from this work was that the acoustic volume velocity was linearly dependent on the valve displacement; hence the interest in reducing the distortion in the valve movement by using the gas bearing.

This paper describes an experimental analysis which has been carried out on a subsonic electropneumatic source built in the laboratory of Acoustics of the Faculté Polytechnique de Mons (Belgium), in collaboration with the Institute of Sound and Vibration Research of the University of Southampton (U.K). The paper is organized as follows. Section 2 describes the design of the subsonic electropneumatic source.

Section 3 is devoted to the presentation and the discussion of the results of the experimental analysis of this source, whereas section 4 deals with the validation of the theoretical model described in the companion paper. Section 5 is concerned with the important issue of the linearization of the source by using a predistortion processor. Finally, the measurement of the pneumatic efficiency of the source is considered in section 6.

2. DESIGN OF A SUBSONIC ELECTROPNEUMATIC SOURCE

The design of a sonic source has been fully discussed by Glendinning *et al*. [2]. In this reference, two different architectures were discussed: the annular sleeve design and the sliding plate design. The annular sleeve design was considered by Fiala *et al*. [3]. An analysis of this type of design reveals that it suffers some major drawbacks: it is difficult to manufacture and assemble the coil and flexure; it is an inflexible design in that the modification of the slot area or shape requires complete re-manufacture of the valve. Moreover the clearance between the stator and the moving parts cannot be varied and turning the flow through 90° causes a reduction in the pressure pulses developed at the slots. The sliding plate design avoids these problems and has the additional advantage that it can be driven by using a standard electrodynamic vibrator. Its main drawback is the pressure loading on the sliding plate, causing high frictional forces and hence limiting the throw of the valve and its linearity. Glendinning *et al*. [2] used an aerostatic thrust bearing to support the plate. In the subsonic case, the relatively small pressure difference between the plenum chamber and the source output section does not seem to necessitate such a heavy and costly solution as the use of low friction materials (PTFE) for the contact surfaces is probably more appropriate.

The main requirements of the subsonic source that was designed in the current work were as follows: frequency range 20–200 Hz. Above this frequency

substantial valve motion is impossible without recourse to an exotic driving mechanism. The plenum pressure should also be only a few hundred Pascals above the atmospheric pressure. Such a low pressure excess allows the source to work in the region where it is the most efficient (but the most non-linear). Another requirement from the source is its flexibility: it has to be designed in such a way that changes in the valve geometry are possible without complete re-manufacture. The driving system chosen was an electrodynamic vibrator (Brüel and Kjaer type 4810), developing a peak force rating of 10 N and a peak-to-peak maximum displacement of 6 mm. This vibrator does not require external cooling. By enclosing the vibrator in the plenum chamber the need for any sliding seals was averted. The vibrator was placed vertically, in order to avoid force imbalance on its suspension. The swept area was chosen to be 48 mm^2. In order to explore the full potential of the transducer at low frquency, i.e., minimize pressure loss through the slots, a slot width of 1 mm was chosen. The final slot arrangement was as follow: 4 slots, length 12 mm, width 1 mm, gap between the slots 1 mm. The slider thickness was chosen equal to 2 mm. Such a thickness was shown to be able [2] to resist pressure loading as large as 3×10^5 Pa. The slot thickness was reduced to 1 mm by milling the centre of the slider, in order to reduce the weight of the slider. A second reason for reducing the slot thickness was aerodynamic and was discussed in Part I: when the slots are aligned, the flow through the port results in a pressure difference between the two sides of the slot, tangential to the flow, and the net force acts to close the valve. The magnitude of this force varies with valve opening position, decreasing as the valve opens and therefore leading to a non-linear behaviour of the valve. This force is dependent on the side area of the slots exposed to the flow so that a reduction in this area causes a corresponding reduction in the axial force and therefore reduces the valve non-linear behaviour. In order to minimize its mass, the slider was constructed in aluminium alloy. The rod connecting the shaker and the slider was chosen to be stiff enough to avoid any transversal movement of the slider, as illustrated in Figure 1. The use of a stiff rod has two drawbacks: it is likely to increase the rod weight and it is unable to

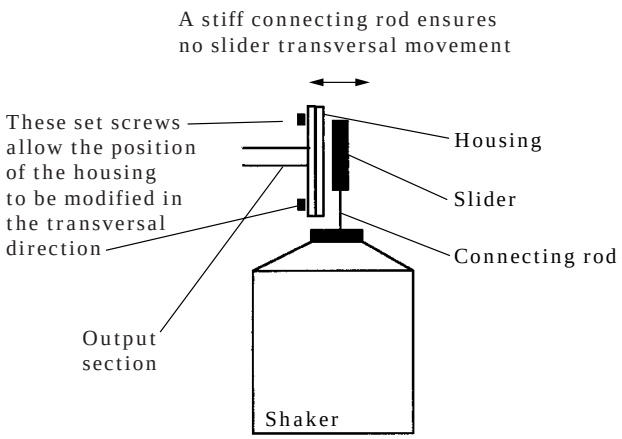

Figure 1. Connecting rod between the slider and the shaker, impeding any slider transversal movement.

accommodate any small misalignment between the vibrator and the slider. However this arrangement has three major advantages: it simplifies the design of the slider housing, that is no longer required to enclose the slider; it allows a reduction of friction between the slider and its housing; and it also allows a fine setting of the clearance between the slider and the housing, by using two screws placed on the housing. The connecting rod was also constructed in aluminium alloy, to reduce weight. The reciprocating mass of the valve, i.e., the mass of the slider and connecting rod, was approximately 8 gm.

For proper operation of the source, the plenum chamber must be large enough to guarantee a constant plenum pressure along the cycle. Assuming the output flow from the source is sinusoidal, one can write

$$Q_{total}(t) = \frac{Q}{2} + \frac{Q}{2}\sin \omega t + \text{leakage flow}, \tag{1}$$

where $Q_{total}(t)$ is the output flow from the source and $Q/2$ is the output flow when the valve is half open. Assuming that the leakage flow, that mainly depends on the clearance between the slider and its housing, is negligible, one can write

$$Q_{total}(t) \cong \frac{Q}{2} + \frac{Q}{2}\sin \omega t. \tag{2}$$

The time average output flow is equal to $Q/2$: the input steady flow in the device is therefore equal to $Q/2$. The volume deficit in the chamber is maximum for $\omega t + \pi$, and is equal to

$$\text{max volume deficit} = \int_0^{\pi} \frac{Q}{2}\sin \omega t \, \mathrm{d}t = \frac{Q}{2}\left[-\frac{\cos \omega t}{\omega} \right]_{\omega t = 0}^{\omega t = \pi} = \frac{Q}{\omega}. \tag{3}$$

The volume deficit is largest at low frequencies. In equation (3), the mean flow rate Q is computed by using the source fundamental equation that was derived in Part I,

$$Q_2(t) = A_1(t)\sqrt{C_d(p_{pl} - p_2(t))/\rho} \tag{4}$$

(the notation being that used in Part I). The minimal volume of the plenum chamber can be assessed by using Boyle's law (an adiabiatic transformation is assumed):

$$p_1 v_1 = p_2 v_2. \tag{5}$$

Here v_2 is the initial volume of the plenum chamber, v_1 is the initial volume of the plenum chamber minus the volume deficit, p_2 is the plenum pressure, and $p_1 = p_2 + \delta p_2$ is the plenum pressure for maximum plenum volume deficit. If the variations of the plenum pressure δp_2 are fixed as 1% of p_2, then one can write

$$(p_2 + p_2/100)(v_2 - Q/\omega) = p_2 v_2. \tag{6}$$

This last equation gives the minimum free volume of the plenum chamber for 1% plenum pressure variation. For the source described here $\bar{A}_1 = 2{\cdot}4 \times 10^{-5}\,\mathrm{m}^2$, $p_{pl} - \bar{p}_2 = 500$ Pa, $\rho = 1{\cdot}2\,\mathrm{kg/m}^3$, $f_{min} = 20$ Hz and $C_d = 2$, from which one can

compute $Q = 0{\cdot}7 \times 10^{-3}$ m^3/s and hence the minimum plenum chamber volume as $v_2 = 101 \times 0{\cdot}7 \times 10^{-3}/(2 \times 20\pi) = 0{\cdot}56$ dm^3.

The plenum chamber external dimensions were chosen as follows: length 290 mm, width 240 mm, height 254 mm. The plenum chamber was made from 18-mm plywood. One side of the chamber was made from transparent plastic to offer the possibility of analyzing the slider movement, by using a stroboscope for example. The plenum chamber free volume was roughly estimated to 10 dm^3 and was therefore largely over-dimensioned compared to the calculation above, but this made the manufacture of the source more practical. Initially, the plenum chamber was supplied with compressed air by using a small compressor (maximum flow rate = 100 l/min), via a 2-m long 53-mm internal diameter circular pipe. The plenum pressure was adjusted by using a small valve at the compressor output. However, initial measurements on the source revealed that it was very difficult to adjust the plenum pressure, the small valve at the compressor output not being very accurate, and so the output flow from the compressor exhibited large fluctuations in time, leading to variations of the plenum pressure throughout the cycle. The compressor was also very noisy and influenced by acoustical measurements. For these reasons, the compressor was replaced by a cylinder of dry air. A pressure reducer was placed at the output of this cylinder. The problems mentioned above then disappeared.

The source output section, located downstream the slider housing, was made from a circular pipe whose dimensions are as follows: length 111 mm, internal diameter 15 mm. It is possible to connect the source to two different ducts. The first one, that will be labelled the 220 × 280-mm duct, is a 3-m long rectangular duct having internal dimensions of the cross-section 220 × 280 mm. An acoustic termination was designed at the end of this duct to minimize the reflection of sound from the far end of the test section but to allow the free escape of air. The second duct has a circular cross-section (diameter 21 mm, length 3 m). This time, because of its small cross-section, no anechoic termination was placed at the duct output.

In order to achieve a sinusoidal, full modulation of the valve, the mean position of the slider must be such that the slots are half open. A first possibility was to use a mechanical system to change the mean slider position. However, a preliminary study revealed that this solution was difficult to implement. For this reason, a controllable d.c. component was added to the electrical voltage feeding the shaker, which allowed the electrical modification of the mean slider position. The shaker was driven by using a 60-W d.c. power amplifier. In order to prevent overheating of the coil of the shaker, an electronic fuse was placed at the output of the power amplifier.

The vertical displacement of the slider versus time, which is proportional to the throat area $A_1(t)$, was measured by using an infrared LED coupled to a receiving diode, as illustrated in Figure 2. The output current of the receiving diode is proportional to the light intensity it receives, which is itself dependent on the slider position. The output current was converted to a voltage that was measured by using an instrumentation amplifier. Preliminary measurements showed that this system was linear for slider peak-to-peak displacements up to 2 mm and that the system was not sensitive to external lighting. The plenum pressure was monitored

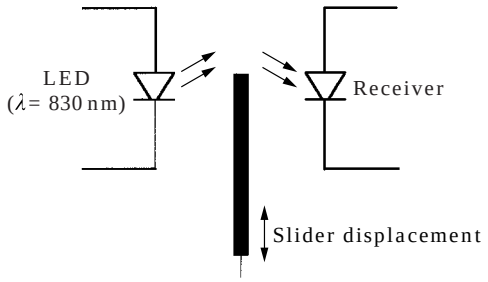

Figure 2. Measurement of the slider position by using a LED and a receiving diode.

by using a small piezo-resistive differential pressure sensor, whose ports respectively vented to the plenum pressure and the ambient pressure. The output of the sensor was connected to a low noise high accuracy instrumentation amplifier. A photograph of the source is shown in Figure 3.

3. EXPERIMENTAL ANALYSIS OF THE TRANSDUCER

3.1. LINEARITY OF THE SLIDER MOVEMENT

The linearity of the slider movement was assessed by measuring the slider displacement versus time for various plenum pressures, by using the optical sensor. The shaker was driven by sine input voltages of various frequencies. The degree of linearity of the slider movement can be assessed via the computation of the harmonic distortion δ_h of its linear displacement $d(t)$, defined as

$$\delta_h(\%) = 100 \frac{\sqrt{A_{2f}^2 + A_{3f}^2 + \cdots + A_{nf}^2}}{\sqrt{A_{1f}^2 + A_{2f}^2 + A_{3f}^2 + \cdots + A_{nf}^2}}, \tag{7}$$

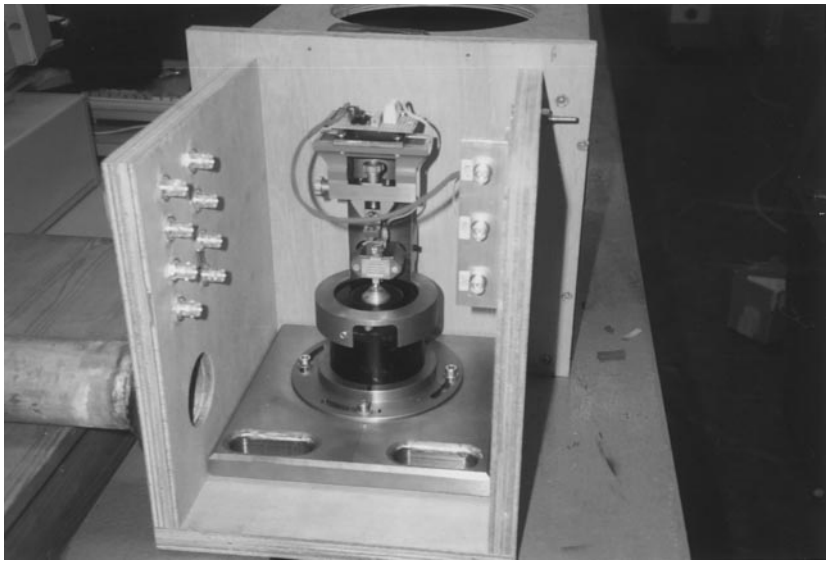

Figure 3. A view of the subsonic electropneumatic source during the assembly phase, showing the vibrator placed in the plenum chamber.

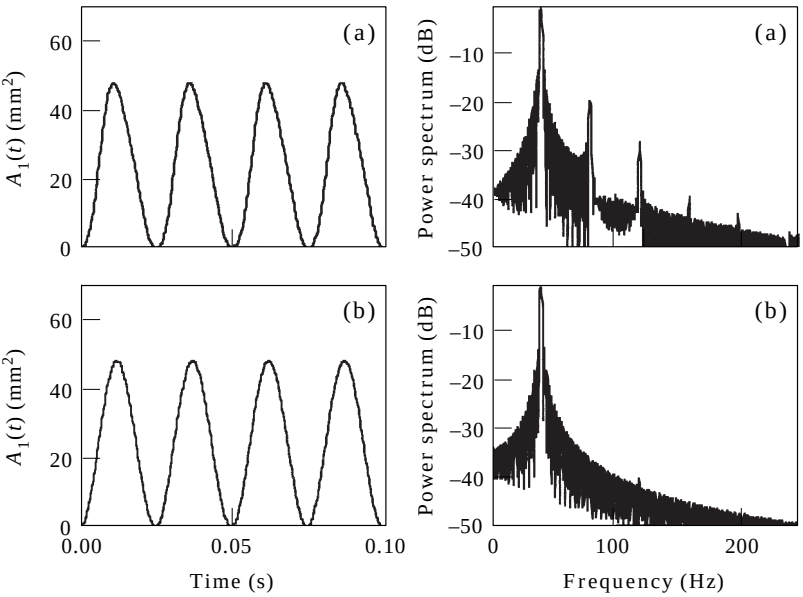

Figure 4. Linearity of the slider movement. (a) Contact between the slider and its housing; (b) no contact between the slider and its housing. Experimental conditions: sinusoidal, full modulation of valve, $f = 40$ Hz, plenum pressure $= p_{atm} + 300$ Pa.

where A_f is the amplitude of the fundamental in the spectrum of signal $d(t)$ and A_{if} is the amplitude of the ith harmonic in this spectrum. The throat area versus time and the power spectrum of this signal are illustrated in Figure 4 for the following experimental conditions: full modulation of valve; frequency 40 Hz, plenum pressure $p_{atm} + 300$ Pa. The harmonic distortion in this case was measured to be 2·5%. Other results showed that the harmonic distortion never exceeds 5%, and was independent of the plenum pressure (at least for the plenum pressures up to $p_{atm} + 500$ Pa). Figure 4 suggests that the main cause of distortion of the slider movement is the friction between the slider and its housing. It was possible to increase the gap between the slider and its housing but this increased the leakage and hence reduced the pneumatic efficiency of the source. Another possible method of reducing friction would be to replace the PTFE coating by an air bearing, but this was not required here since the residual distortion with the PTFE coating was felt to be acceptable.

3.2. ACOUSTIC PRESSURE AT THE SOURCE OUTPUT

The acoustic pressure at the source output was measured in various experimental conditions, by using the experimental set-up of Figure 5. This system allows the measurement of both the slider displacement and the acoustic pressure at the source output. The acoustic pressure was measured by using a pressure microphone. Measurements were carried out for various frequencies ranging from 20 to 120 Hz, and for various plenum pressures up to 300 Pa. In a first set of experiments, the source was connected to the 220 × 280-mm duct. The position of the measurement microphone with respect to the source output is illustrated

in Figure 5, and Figure 6 illustrates a typical result. The frequency of the sine wave generator was set to 56 Hz, which is a particulary interesting frequency because the response of the 220 × 280-mm duct is almost identical for both the fundamental, the second harmonic (112 Hz), the third harmonic (168 Hz) and the fourth harmonic (224 Hz). The distortion in the signal $p_2(t)$ at this frequency is thus hardly influenced by the duct and is only due to the source. The harmonic content of the acoustic pressure $p_2(t)$ is quite similar to that of the signal $A_1(t)$ in this case, which suggests that the main source of non-linearities in the system is the slider movement. The phenomenon of pressure equalization expected from the theoretical analysis does not appear to occur. The magnitude of acoustic pressure fluctuations at the source output is, however, only equal to a few percent of the excess pressure in the plenum chamber. The situation is different when the source is connected to the 21-mm duct, in which case the results of the measurements are illustrated in Figure 7. Once again a frequency was chosen for which the duct had almost no influence on the waveform at the source output. The phenomenon of equalization now clearly appears, and the magnitude of acoustic pressure fluctuations at the source output is almost equal to the excess pressure in the plenum chamber. This preliminary experimental analysis demonstrated the effect of the acoustic load impedance on the output waveform of the source. This effect is also demonstrated in the theoretical analysis since the smaller the acoustic impedance seen by the source, the smaller the acoustic pressure variations at the source output. In this case, the fundamental equation of the subsonic source

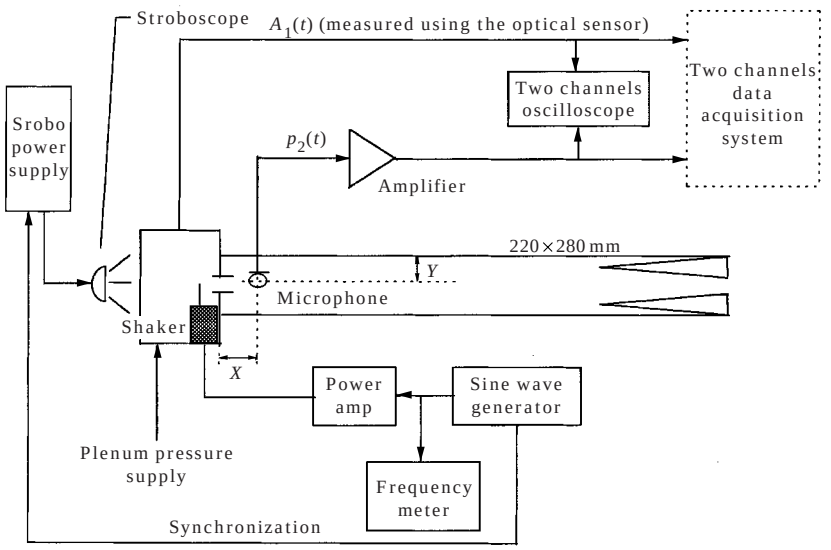

Figure 5. Measurement of the acoustic pressure at the output of the subsonic electropneumatic source. For each measurement, a sinusoidal, full amplitude modulation of the valve was achieved. The valve movement was controlled by using a stroboscope. For convenience, the differential pressure sensor for measuring the plenum pressure is not illustrated in the figure. The acoustic pressure at the source output was measured by using a pressure microphone located as follows: (a) source connected to the 220 × 280-mm duct, $X = 9$ cm, $Y = 7$ cm; (b) source connected to the 21-mm duct, $X = 20$ cm; $Y = 0{\cdot}5$ cm.

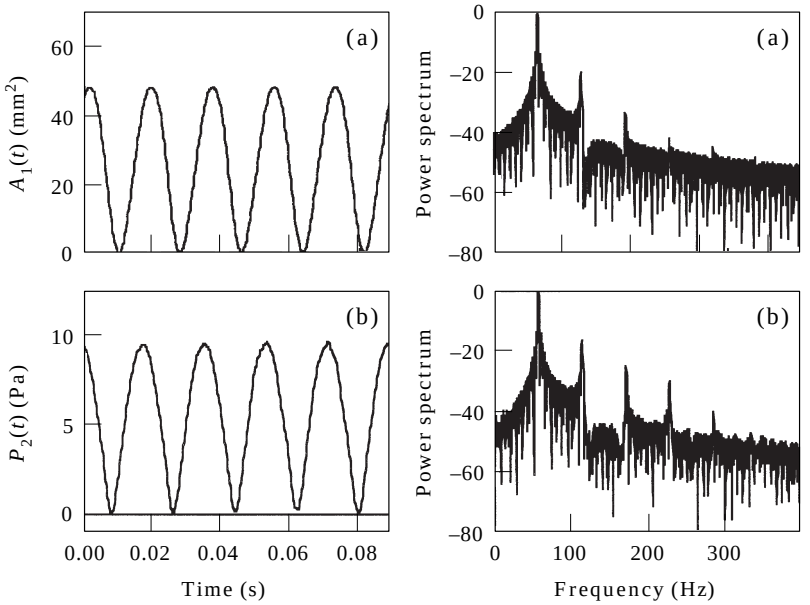

Figure 6. Acoustic response of the subsonic source. Experimental conditions: $f = 56$ Hz, $p_{pl} = p_{atm} + 150$ Pa. Source connected to the 220 × 280-mm duct. (a) Throat area versus time and power spectrum of this signal; (b) acoustic pressure at the source output and power spectrum of this signal. The d.c. part of this signal was measured by using the differential pressure sensor described in section 2. Ports of this device respectively vented to the ambient pressure and to a location close to the microphone of Figure 5.

(equation (4)) becomes almost linear since $p_{pl} - p_2(t)$ is close to p_{pl}, which is a constant. The production of sound is rather inefficient if the source is operated in this mode, however. If the system is to have large efficiency, the load resistance must be large compared to the resistance of the throat opening, since the acoustic power derived by the source is the power dissipated in this radiation resistance.

4. VALIDATION OF THE THEORETICAL MODEL

In the theoretical analysis of Part I, an equation was given for the prediction of the volume velocity at the output of the subsonic electropneumatic source (equation (4) of this paper). The accuracy of this theoretical model was examined experimentally. Initial experiments were conducted to determine the optimal value of the discharge coefficient C_d. The procedure for the estimation of the optimal discharge coefficient $C_{d,opt}$ can be described as follows, with reference to Figure 8. In this figure, $p_{2th}(t)$ is the "theoretical" value of $p_2(t)$ if equation (4) is valid and is defined as

$$p_{2th}(t) = \left(aA_1(t) \sqrt{\frac{p_{pl} - p_{2mes}(t)}{\rho}} \right) * z_a(t), \tag{8}$$

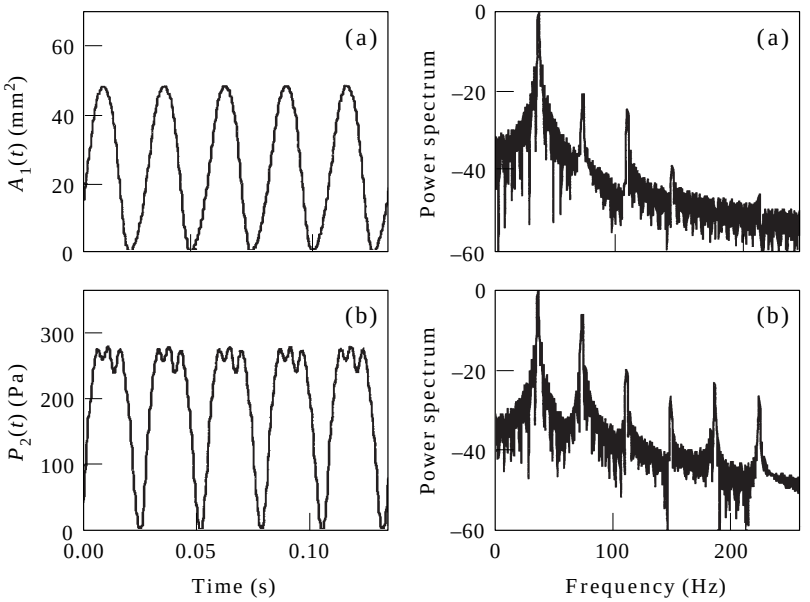

Figure 7. Acoustic response of the subsonic electropneumatic source. Experimental conditions: $f = 37$ Hz, $p_{pl} = p_{atm} + 300$ Pa. Source connected to the 21-mm duct. (a) Throat area versus time; power spectrum of this signal; (b) acoustic pressure at the source output; power spectrum of this signal.

where $a = \sqrt{C_d}$ is the square root of the discharge coefficient, $*$ is the convolution operator, $z_a(t)$ is the impulse response of the duct to which the source is connected, and $p_{2mes}(t)$ is the measured value of the acoustic pressure at the source output.

The computation of $p_{2th}(t)$ requires the measurement of $A_1(t)$ and $(p_{pl} - p_{2mes}(t))$ and the estimation of $z_a(t)$, the impulse response of the duct. The optimal value of coefficient a, a_{opt}, is the value that mlinimizes the cost function J, defined as

$$J = E[(p_{2th}(t) - p_{2mes}(t))^2], \tag{9}$$

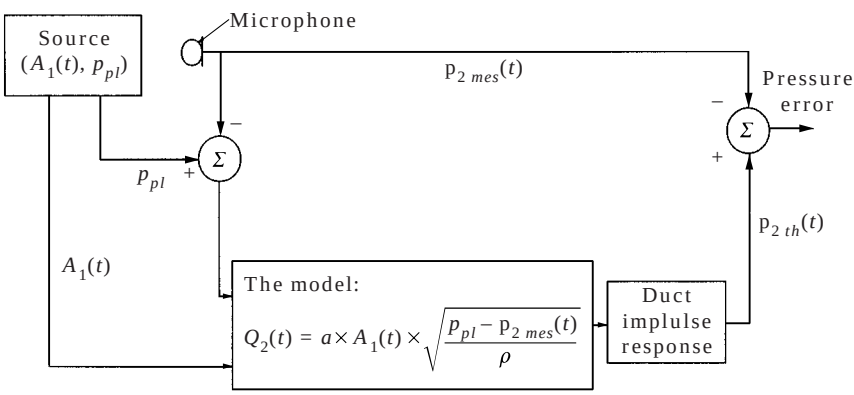

Figure 8. Determination of the optimal discharge coefficient. Block diagram.

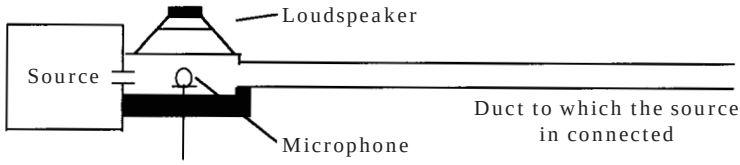

Figure 9. Experimental set-up for measuring the acoustic input impedance of the duct (220 × 280-mm or 21-mm duct) to which the source is connected.

in which E is the mean value operator. Upon defining the function $f(t)$ as

$$f(t) = \left(A_1(t) \sqrt{\frac{p_{pl} - p_{2mes}(t)}{\rho}} \right) * z_a(t) \tag{10}$$

then equation (9) can be written by using equation (8),

$$J = a^2 E[(f(t))^2] - 2aE[(f(t)p_{2mes}(t))] + E[(p_{2mes}(t))^2]. \tag{11}$$

The optimum value of a is the value for which the derivative of J with respect to a is equal to zero. After derivation of equation (11) one finds

$$a_{opt} = E[f(t)p_{2mes}(t)]/E[(f(t))^2]. \tag{12}$$

The optimal discharge coefficient $C_{d,opt}$ is then the square of a_{opt}. The validity of the theoretical model can be estimated by computing the correlation coefficient K between functions $p_{2mes}(t)$ and $p_{2th}(t)$, defined as follows if zero mean processes are assumed (see for example reference [4]):

$$K = \frac{E[p_{2th}(t)p_{2mes}(t)]}{\sqrt{E[p_{2th}(t)^2]}\sqrt{E[(p_{2mes}(t))^2]}}. \tag{13}$$

The closer this coefficient is to 1, the more accurate the theoretical model can be assumed to be. The validation of the theoretical model requires the estimation of the acoustic impedance and of the impulse response of the duct to which the source is connected. The source output was slightly modified to allow this measurement, as illustrated in Figure 9. The loudspeaker was fed with white noise and the linear velocity of the diaphragm, $v(t)$, was measured with an accelerometer. The acoustic pressure in front of the loudspeaker, $p(t)$, was also measured by using a microphone. The slider was arranged to be completely closed for these measurements. If $V(\mathrm{j}\omega)$ and $P(\mathrm{j}\omega)$ are the Fourier transforms of the signals $v(t)$ and $p(t)$, then the acoustic impedance $Z_a(\mathrm{j}\omega)$ at the entrance of the duct can be calculated as

$$Z_a(\mathrm{j}\omega) = P(\mathrm{j}\omega)/SV(\mathrm{j}\omega), \tag{14}$$

where S is the area of the loudspeaker diaphragm. The impulse response of the duct is the inverse Fourier transform of $Z_a(\mathrm{j}\omega)$. The impulse responses of both the 220 × 280-mm duct and of the 21-mm duct were measured in this way. The impulse response of the 220 × 280-mm duct is shown in Figure 10. Because of the acoustic termination at the end of this duct, the impulse response is reasonably well damped.

In the experiments $A_1(t)$ was measured by using the optical sensor, p_{pl} by using the differential pressure sensor, and $p_{2mes}(t)$ by using the microphone. For all the measurements, a sinusoidal modulation of the valve was achieved. By using the impulse response of the duct and the measured signals $A_1(t)$ and $p_{2mes}(t)$, the function $f(t)$ was computed by using equation (10). The optimal coefficient a_{opt} is then computed by using equation (12). The signal $p_{2th}(t)$ is then computed by using equation (8). Finally, the coefficient of correlation K between $p_{2th}(t)$ and $p_{2mes}(t)$ is computed (equation (13)). This procedure was carried out for various frequencies up to 100 Hz and for vairous d.c. plenum pressures. Figures 11(a,b) present some typical results. The optimal discharge coefficient calculated for various driving frequencies and plenum pressures is illustrated in Figure 12. This coefficient was measured when the source was connected to both the 21-mm duct and the 220 × 280-mm duct described in section 2. No major difference in the discharge coefficient was noticed between these two cases. The discharge coefficient is close to 2, a result that was derived theoretically by Sivian [5], Clark Jones [6] and Ingard and Ising [7]. According to Sivian's work, this value of the discharge coefficient shows that the flow across the orifice is fully turbulent. The assumption used in the theoretical analysis of a constant discharge coefficient of 2 is thus seen to be reasonably well validated by the experimental investigation, under a wide variety of conditions. The fundamental equation of subsonic compressed-air sources derived in the theoretical analysis can thus be taken as a good model for explaining the behaviour of the subsonic electropneumatic source. The coefficient of correlation between the predicted pressure and the measured pressure was larger than 0·9 in every case, which again suggests that the theoretical model is a good one, particularly if one takes into account the various sources of error in the procedure of validation. These include the error in the measurement of the duct acoustic impedance, the error in the measurement of the source output

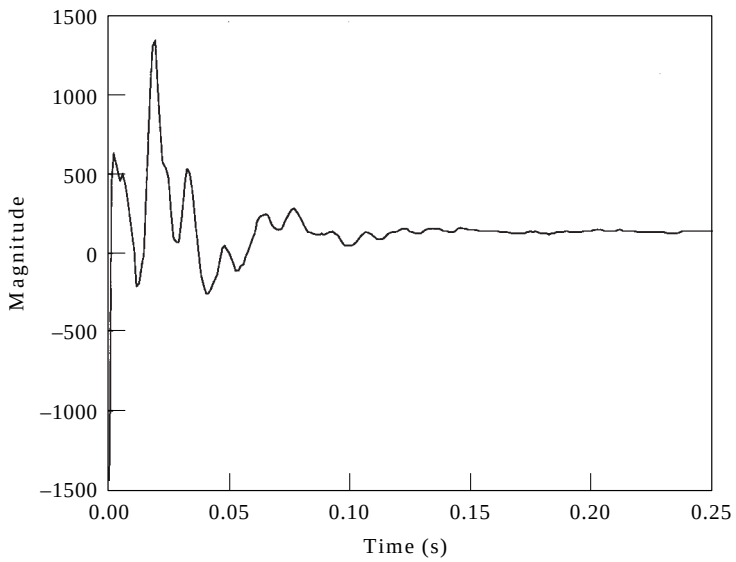

Figure 10. Impulse response of the 220 × 280-mm duct.

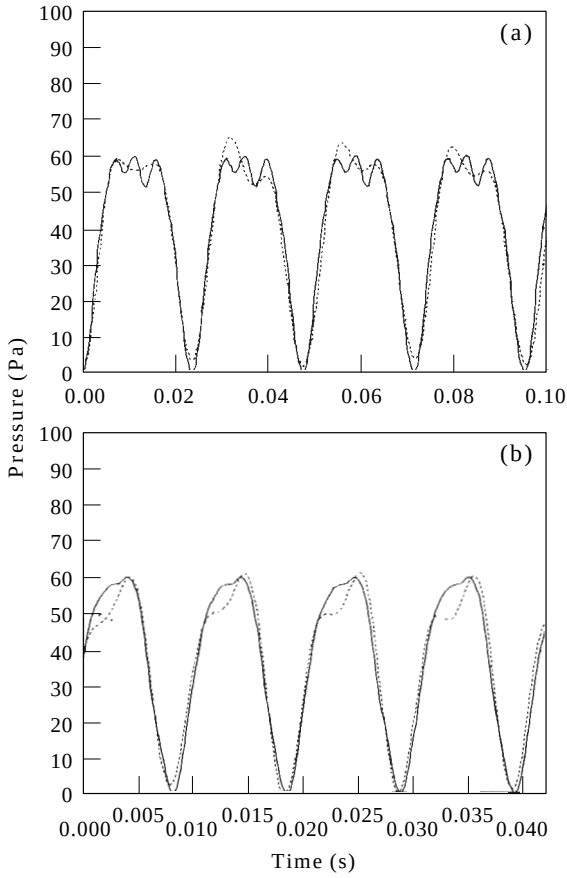

Figure 11. Comparison of the measured acoustic pressure (– – – –) with the acoustic pressure computed by using the model (——). The source was connected to the 21-mm duct. Experimental conditions are as follows: (a) sinusoidal, full modulation of valve, $p_{pl} = p_{atm} + 60$ Pa, $f = 37$ Hz; (b) sinusoidal, full modulation of valve, $p_{pl} = p_{atm} + 60$ Pa, $f = 86$ Hz.

acoustic pressure, in the measurement of $A_1(t)$ and in the measurement of the plenum pressure.

5. PREDISTORTION OF THE SOURCE

Pressure equalization was shown in the theoretical analysis to be the main cause of non-linearity in the subsonic source. The linearization of such a source has been discussed by Allen and Watters [8], whose purpose was to control the waveform at the output of an acoustic siren, a device that was demonstrated to have a similar behaviour to that of the subsonic compressed air source. Allen and Watters demonstrated that although the siren was non-linear, it was still possible to generate a sinusoidal wave by varying the open area of the siren port in a non-sinusoidal way. They proposed an analytic expression to compute the time variation of the port area leading to the generation of a sinusoidal waveform. This time variation of area was designed into the stator port shape. The experimental

results demonstrated that the output waveform was almost perfectly sinusoidal: harmonics were more than 20 dB below the fundamental over a wide range of plenum pressures. The main drawback of the Allen and Watters siren is that the production of other than a sinusoidal waveform requires a complete re-manufacture of the stator of the siren. In the subsonic electropneumatic source the throat area versus time is controlled by the electrical current feeding the electrodynamic shaker, which offers more flexibility. In the theoretical analysis of Part I an equation was derived that gives the throat area versus time for the production of a required pressure $p_{2required}(t) = A \sin(2\pi ft)$, which is

$$A_1(t) = K \sin\{2\pi f(t-\theta)\} \frac{1}{\sqrt{p_{pl} - \{A \sin(2\pi ft)\}}}, \tag{15}$$

where K is a constant and θ is a time delay which is a function of the phase angle of the acoustic impedance of the duct to which the source is connected at frequency f. Equation (15) suggests that, in practice, the required throat area can be computed by using the following procedure: (a) the plenum pressure p_{pl} is measured by using the pressure sensor described in section 2; (b) the pressure $p_{2required}(t)$ is defined by $p_{2required}(t) = A \sin(\omega t)$; (c) the difference between the plenum pressure and the required pressure is computed as $u(t) = p_{pl} - p_{2required}(t)$; (d) the square root of the signal $u(t)$ is computed, to produce the signal $s(t)$; (e) the inverse of signal $s(t)$ is computed, producing signal $i(t)$; (f) the signal $i(t)$ is multiplied by the signal $d(t)$, a delayed version of signal $p_{2required}(t)$, $v(t) = i(t)d(t)$, with $d(t) = p_{2required}(t - \theta)$; (g) the signal $u(t)$ is sent to the power amplifier and then to the shaker. This process of linearization is an open loop procedure whose

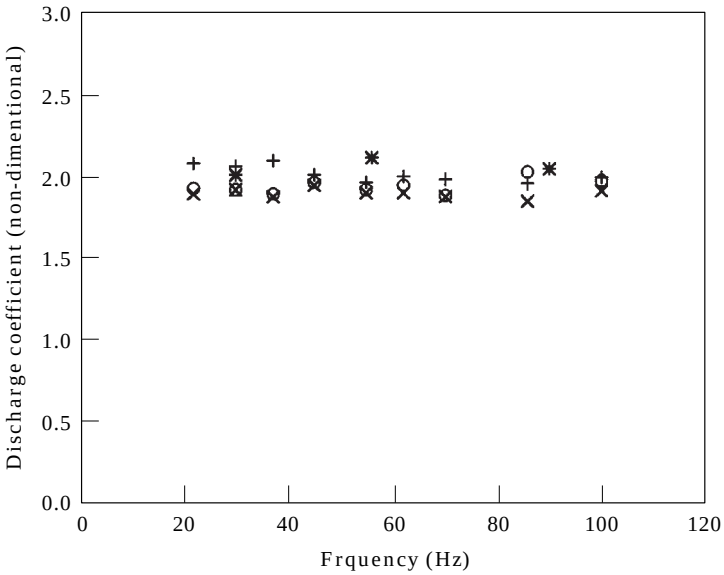

Figure 12. Optimal discharge coefficient versus driving frequency and plenum pressure. +, 21-mm duct, $p_{pl} = 60$ Pa above atmospheric pressure; ○, 21-mm duct, $p_{pl} = 150$ Pa above atmospheric pressure; ×, 21-mm duct, $p_{pl} = 300$ Pa above atmospheric pressure; ∗, 220 × 280-mm duct, $p_{pl} = 150$ Pa above atmospheric pressure.

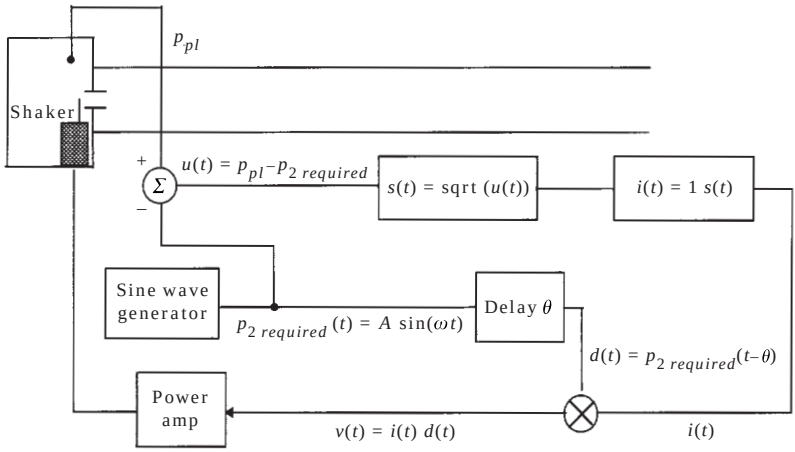

Figure 13. Open loop linearization of the subsonic compressed-air source. Block diagram.

block-diagram is illustrated in Figure 13. The various operations were implemented on a Texas Instruments TMS320C25 signal processing board, programmed by using the assembler language. In order to check the accuracy of the predistortion system, the acoustic pressure at the source output was measured by using the arrangement of Figure 14. For each of these measurements, a

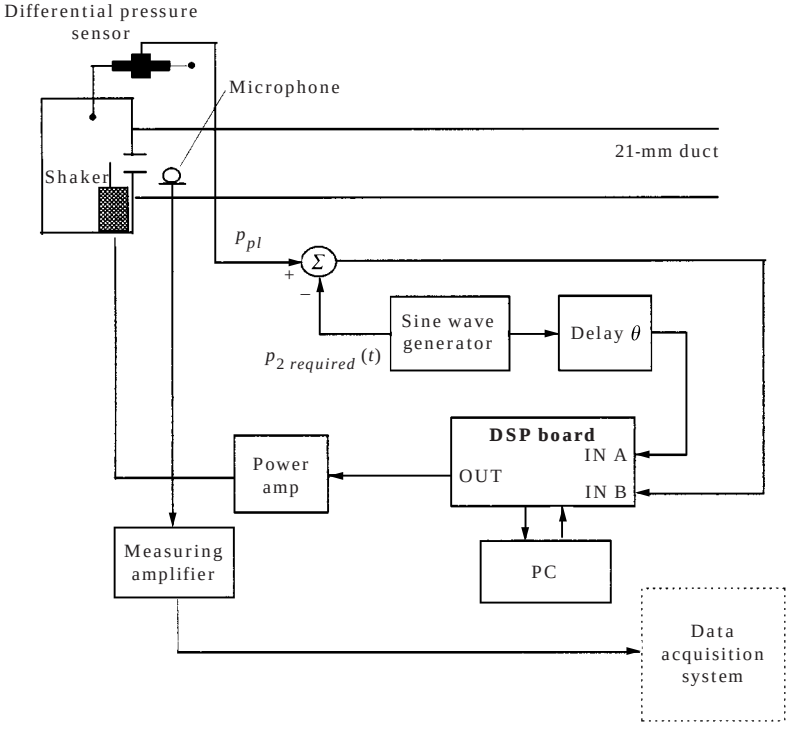

Figure 14. Experimental arrangement for the linearization of the subsonic compressed-air source.

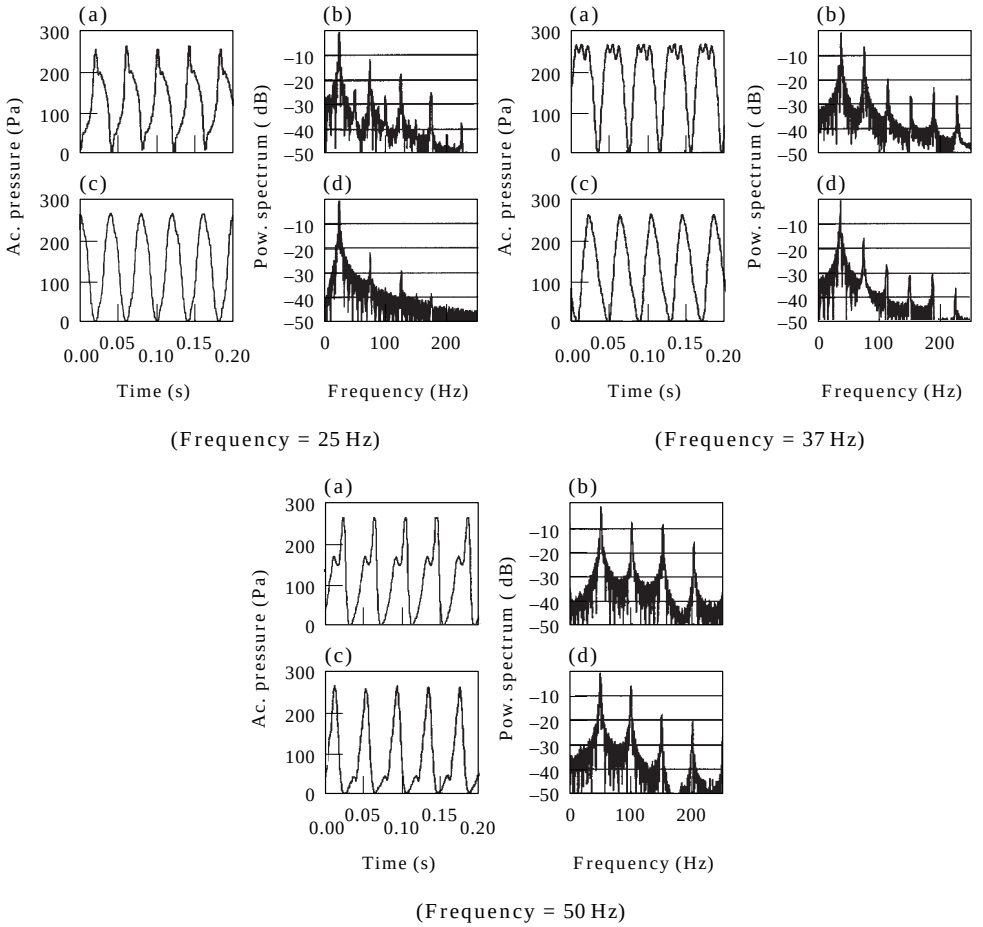

Figure 15. Linearization of the subsonic compressed air source. The experimental conditions are described in the text. (a) Acoustic pressure versus time at the source output when the slider has a sinusoidal movement; (b) power spectrum of this signal; (c) acoustic pressure versus time at the source output when the source is linearized; (d) power spectrum of this signal.

sinusoidal acoustic pressure at the source output was required and a full modulation of the source was achieved. The plenum pressure was 300 Pa above the atmospheric pressure. To assess the effect of predistortion, the measured acoustic pressures at the source output was compared with the acoustic pressures achieved for a sinusoidal movement of the slider. This comparison is illustrated for three frequencies in Figure 15. This figure shows that the predistortion processor is reasonably successful in linearizing the subsonic electropneumatic source, particularly for low frequencies. The degree of linearization at the source output however quickly decreases when the frequency increases and at $f = 50$ Hz the method of predistortion is not very efficient. The cause of this failure is to be found in the poor frequency response of the mechanical part of the subsonic compressed air source, which falls off rapidly above 45 Hz. For this reason it does not seem possible to linearize the source for frequencies larger than, say, 40–45 Hz by using the arrangement shown in Figure 14. The frequency response of the slider

could be improved by reducing its weight or increasing the stiffness of the shaker, and the linearization method outlined above could then be operated up to higher frequencies. Alternatively the frequency response of the slider could be compensated for within the processor used in the linearizer shown in Figure 14, although this possibility has not been investigated in practice.

6. EFFICIENCY OF THE SOURCE

The pneumatic efficiency of electropneumatic sources was defined in Part I. A thermodynamic method of measuring the pneumatic efficiency was proposed by Clark Jones [6]. The method is based on the assumption that the only form of energy, other than heat, into which the available energy of the air stream is converted, is acoustical energy. If all the available energy were used in this fashion, the temperature of the exhausted air would be less than the temperature of the air in the chamber by the amount corresponding to an adiabatic, reversible expansion from the chamber pressure to atmospheric pressure. Thus, the pneumatic efficiency of the source is the ratio of the measured temperature difference to that corresponding to an adiabatic reversible expansion between the two pressures. A similar result was used to measure the efficiency of a turbine. The basic quantity to be measured is therefore the difference between the temperature of the air immediately below and above the slider. The analysis of turbine operation and of modulation shows that the physics of the systems is quite different however. This difference was explicitly noticed by Mitchell and Muster [9]. The second method for measuring the pneumatic efficiency of the subsonic compressed air source is the direct method, in which both the source pneumatic input power and acoustic output power are measured, and this was the method adopted here.

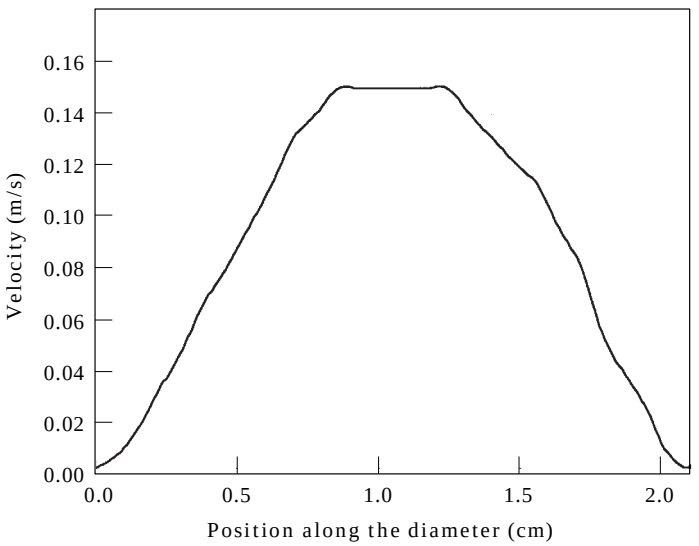

Figure 16. Velocity profile along one diameter of the cross-section of the 21-mm duct. Frequency = 47 Hz, plenum pressure = p_{atm} + 50 Pa.

TABLE 1

Measurement of the pneumatic efficiency of the subsonic electropneumatic source: *experimental results*; (1) *given above the atmospheric pressure*; (2) *reference* 2×10^{-5} Pa; (3) *computed by using the following values for the acoustic load resistance*: $R_l = 2{\cdot}44 \times 10^6$ Ns/m^5 ($f = 47$ Hz); $R_l = 4{\cdot}88 \times 10^6$ Ns/m^5 ($f = 52$ Hz); *and* $R_l = 4{\cdot}63 \times 10^6$ Ns/m^5 ($f = 95$ Hz); (4) *sound power level at* 20 *cm from the source output*, *reference* 10^{-12} *W*

Frequency (Hz)	Plenum pressure (1)	SPL (dB) (2)	Acoustic power (W) (3)	Power level (dB) (4)	Flow (m^3/s)	Pneumatic power (W)	Pneumatic efficiency (%)
47	50	125	$5{\cdot}18 \times 10^{-4}$	87	$2{\cdot}18 \times 10^{-5}$	$1{\cdot}09 \times 10^{-3}$	47·5
	150	134	$4{\cdot}12 \times 10^{-3}$	96	$5{\cdot}71 \times 10^{-5}$	$8{\cdot}53 \times 10^{-3}$	48
	350	141	$2{\cdot}06 \times 10^{-2}$	103	$1{\cdot}21 \times 10^{-4}$	$4{\cdot}23 \times 10^{-2}$	48
52	50	117	$4{\cdot}11 \times 10^{-4}$	86	$2{\cdot}20 \times 10^{-5}$	$1{\cdot}10 \times 10^{-3}$	37
	150	126	$3{\cdot}26 \times 10^{-3}$	95	$5{\cdot}76 \times 10^{-5}$	$8{\cdot}63 \times 10^{-3}$	38
	350	131	$1{\cdot}03 \times 10^{-2}$	100	$1{\cdot}20 \times 10^{-4}$	$4{\cdot}17 \times 10^{-2}$	25
95	50	127·5	$4{\cdot}86 \times 10^{-4}$	87	$2{\cdot}21 \times 10^{-5}$	$1{\cdot}11 \times 10^{-3}$	44
	150	135·5	$3{\cdot}86 \times 10^{-3}$	96	$5{\cdot}93 \times 10^{-5}$	$8{\cdot}91 \times 10^{-3}$	43·5
	350	143	$1{\cdot}72 \times 10^{-2}$	102	$1{\cdot}18 \times 10^{-4}$	$4{\cdot}13 \times 10^{-2}$	42

6.1. MEASUREMENT OF THE ACOUSTIC POWER

When the source is connected to a purely resistive acoustic load, the acoustic power can be estimated by measurement of the rms value of the acoustic pressure at a position close to the source output. The acoustic power was thus measured only at frequencies for which the acoustic load was purely resistive. The source was connected to the 21-mm duct, and the microphone was placed in a position similar to that given in Figure 5.

6.2. MEASUREMENT OF THE PNEUMATIC POWER

The pneumatic power can be estimated via the measurement of the plenum pressure p_{pl} and of the d.c. flow $\bar{u}_1 \bar{A}_1$. The flow across the source was measured by using a hot wire anemometer. The hot-wire probe was placed 0·5 cm away from the output of the 21-mm duct and the velocity of air was measured every 0·1 cm along only one diameter of the duct cross-section. This methodology was justified by preliminary measurements that showed that the velocity of air was independent of the diameter chosen (laminar flow). The flow Q across the system was computed from the equation

$$Q = \bar{u}_1 \bar{A}_1 = \int\int_S u(S)\, \mathrm{d}S, \tag{16}$$

where S is the area of the cross-section of the duct and $u(S)$ is the d.c. component of the velocity of air at various positions of this cross-section.

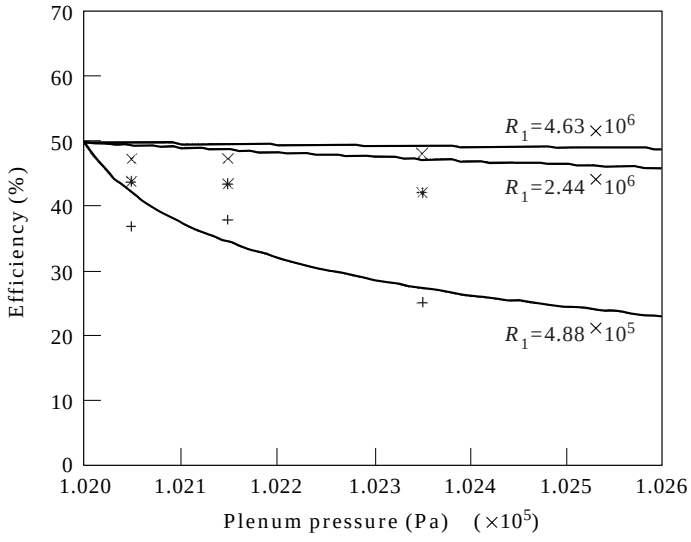

Figure 17. Pneumatic efficiency of the subsonic source for various experimental conditions, ×, $f = 47$ Hz (load resistance $2{\cdot}44 \times 10^6$ N/m^5); +, $f = 52$ Hz (load resistance $4{\cdot}88 \times 10^5$ N/m^5); ∗, $f = 95$ Hz (load resistance $4{\cdot}63 \times 10^6$ N/m^5). For comparison, solid lines give the pneumatic efficiency computed in the theoretical analysis. Values of the acoustical loads R_1 on these curves are in Ns/m^5.

6.3. EXPERIMENTAL RESULTS

The frequencies chosen for the measurements were 47, 52 and 95 Hz, for which the input impedance of the duct was almost entirely real and was equal to $2{\cdot}44 \times 10^6$ Ns/m^5, $4{\cdot}88 \times 10^5$ Ns/m^5 and $4{\cdot}63 \times 10^6$ Ns/m^5, respectively. To ensure a fair comparison between the theoretical and the experimental results, the source was connected to the predistortion processor, in order to produce an acoustic pressure which was as close as possible to a sine wave.

The sound pressure level at the source output and the velocity profile along a diameter of the cross-section of the duct were measured for three different plenum pressures: $p_{atm} + 50$ Pa, $p_{atm} + 150$ Pa and $p_{atm} + 350$ Pa. The throat area was fully modulated. A typical velocity profile is illustrated in Figure 16. From the measurements the acoustic power at the source output, the flow across the source, the pneumatic power required to feed the source with compressed air and the source pneumatic efficiency were successively computed. Table 1 summarizes the results and Figure 17 gives a plot of the pneumatic efficiency calculated from the measured data in the conditions described above. The measured pneumatic efficiencies depend on the source load resistance and slightly decrease as the plenum pressure increases. The measured efficiencies are in reasonably good agreement with the theoretical prediction from Part I, which are also shown in Figure 17. The additional losses encountered in the experimental source can be attributed to several causes, including the air leakage, the backward radiation into the plenum chamber, the losses due to turbulence at the throat and the losses through the walls of the duct to which the source is connected. There are also several possible causes of error in the experimental determination of the pneumatic efficiency of the subsonic source which include the distortion in the acoustic pressure signal, which is particularly prevalent at 95 Hz, and the effect of the air flow on the measurement of the acoustic pressure, which affected all the measurements to the same extent.

7. CONCLUSIONS

A subsonic compressed air source has been constructed to test the validity of the theoretical analysis developed in Part I. The device was originally designed to work up to 200 Hz, but the dynamics of the shaker used to drive the slider prevented reliable operation above about 100 Hz. The valve movement was measured with an optical detector and found to be a linear fraction of the input voltage to the shaker. As expected, the mechanism of sound production in subsconic sources is found to be non-linear and is subject to the phenomenon of equalization between the plenum chamber and the source output section. The experimental results are in good agreement with the theoretical model derived in the companion paper. The source was also linearized by using a predistortion processor which worked reasonably well for frequencies up to 45 Hz, say. The problem with this procedure at higher frequencies was the limited frequency response of the moving system which comprised the shaker, the slider and the housing. The pneumatic efficiency of the source was also measured at several frequencies for which the acoustic load was purely resistive. Pneumatic efficiency

ranges between 25 and 50% and is found to be in reasonable agreement with that predicted from the theoretical analysis. The subsonic compressed air source designed is thus confirmed as being a relatively efficient sound generator since for small plenum pressure excess, their pneumatic efficiency is close to the theoretical maximum pneumatic efficiency for sine waves which is 50%. The use of the subsonic source as a secondary actuator in active noise control systems is currently being investigated.

ACKNOWLEDGMENT

The authors gratefully acknowledge Mr R. Quennay and the mechanics unit of the Faculté Polytechnique de Mons for the construction of the subsonic electropneumatic source, as well as Mr P. Lecomte, technician in the laboratory of acoustics of the Faculté Polytechnique de Mons, who designed most of the electronic equipment described in this paper.

REFERENCES

1. A. G. Glendinning, P. A. Nelson and S. J. Elliott 1990 *Journal of Sound and Vibration* **138**, 479–491. Experiments on a compressed air loudspeaker.
2. A. G. Glendinning, S. J. Elliot and P. A. Nelson 1988 *ISVR Technical Report* 156, *University of Southampton*, *U.K.* A high intensity acoustic source for active attenuation of exhaust noise.
3. W. T. Fiala, J. K. Hilliard, J. A. Renkus and J. J. Van Houten 1966 *Journal of the Acoustical Society of America* **38**, 956–964. Electropneumatic acoustic generator.
4. P. A. Nelson and S. J. Elliott 1992 *Active Control of Sound*. London: Academic Press.
5. L. J. Sivian 1935 *Journal of the Acoustical Society of America* **7**, 94–101. Acoustic impedance of small orifices.
6. R. Clark Jones 1946 *Journal of the Acoustical Society of America* **18**, 371–387. A fifty horse power siren.
7. U. Ingard and H. Ising 1967 *Journal of the Acoustical Society of America* **42**, 6–17. Acoustic nonlinearity of an orifice.
8. C. H. Allen and B. G. Watters 1957 *Journal of the Acoustical Society of America* **31**, 463–469. Siren design for producing controlled wave form with amplitude modulation.
9. W. S. Mitchell and D. Muster 1969 *Journal of the Acoustical Society of America* **45**, 83–91. Evaluation of the acoustic response of an air–water siren.